

University of Minnesota Supercomputer Institute Research Report UMSI 94/202

UMSI 94/202 October 1994

**NUMERICAL STUDIES OF LANGEVIN
EQUATIONS FOR THE DYNAMICS
OF A DENSE HARD SPHERE FLUID**

Oriol T. Valls and Chandan Dasgupta

1200 Washington Avenue South □ Minneapolis, Minnesota 55415

NUMERICAL STUDIES OF LANGEVIN
EQUATIONS FOR THE DYNAMICS OF A DENSE
HARD SPHERE FLUID

Oriol T. Valls*

School of Physics and Astronomy

and Minnesota Supercomputer Institute

University of Minnesota, Minneapolis, Minnesota 55455

Chandan Dasgupta

Department of Physics, Indian Institute of Science

and Jawaharlal Nehru Center for Advanced Scientific Research

Bangalore 560012, India

Abstract

We review numerical results obtained by deriving and solving a set of Langevin equations corresponding to a hard sphere system. We present results showing the different relaxation regimes that are found to exist at moderately high densities, and the different time scales that influence the behavior of the system at higher densities. The results are discussed in connection with those from experiments, molecular dynamics simulations, and mode coupling theory.

I. INTRODUCTION

When a liquid is cooled to temperatures below the equilibrium freezing temperature at a rate which is sufficiently fast to prevent crystallization, it enters a metastable supercooled state. The dynamic behavior of a liquid in this state exhibits many interesting features^{1,2}, the most prominent among them being a rapid growth of the characteristic relaxation time, as reflected in a large number of experimentally measured quantities such as viscosity and dielectric relaxation. Angell has proposed² a classification of supercooled liquids into two categories on the basis of the form of the temperature dependence of the viscosity. Liquids for which the viscosity exhibits a simple Arrhenius form of growth are called "strong" in this scheme, whereas liquids called "fragile" are those in which the viscosity exhibits a faster-than-Arrhenius growth as the temperature is lowered. This non-Arrhenius growth of the viscosity (and other quantities, such as the inverse diffusion constant, which characterize the time scales of relaxation processes) in fragile liquids has been a subject of much experimental, numerical and theoretical investigation. Another interesting feature of the dynamics of fragile liquids in the supercooled state is non-Debye relaxation. Experiments and simulations show that certain time-dependent correlation functions of such a liquid do not show a simple exponential decay in time. One generally finds a complicated form of relaxation with several distinct regimes characterized by different forms of the decay in time. At sufficiently low temperatures, the viscosity becomes so large that the system behaves like a disordered solid for most purposes. This state of matter is called a glass. The glass transition temperature T_g is conventionally defined as the temperature at which the viscosity reaches a value of 10^{13} P.

In spite of extensive efforts spanning several decades, a complete understanding of the dynamics of dense supercooled liquids near the glass transition is not yet available. In recent years, considerable progress in this direction has been achieved through the development of so-called mode coupling (MC) theories³ of the glass transition. In MC theories, the slowing down of the dynamics near the glass transition is attributed to a nonlinear feedback mechanism arising from correlations of density fluctuations in the liquid. The existence of this feedback mechanism was first pointed out by Leutheusser⁴ who proposed, on the basis of detailed kinetic theory calculations, an approximate equation for the decay of time-dependent correlation functions of the liquid which predicted a divergence of the relaxation time at a characteristic "ideal glass transition" temperature. Similar results were independently obtained by Bengtzelius, Götze and Sjolander⁵ at about the same time. The kinetic theory approach to the MC description has been subsequently generalized and

extended by Götze and co-workers^{6,7}. A description very similar to the one obtained from the kinetic theory approach has also been derived^{8,9} from a perturbative treatment of the equations of nonlinear fluctuating hydrodynamics (NFH)¹⁰ which describe the dynamics of the liquid in terms of Langevin-type equations for a small number of “hydrodynamic” variables such as number density and current density. Initial calculations within the MC framework did not take into account the details of the equilibrium short-range structure of the dense liquid. For this reason, these calculations did not lead to reliable predictions for the wavenumber dependence of the relaxation. More recent studies^{9,11,12} have attempted to incorporate information about liquid structure in the MC description of the kinetics.

As mentioned above, the original version of MC theories^{4,5} predicted a power-law divergence of the characteristic time scales of the liquid at an “ideal glass transition” temperature T_c . Experimental and numerical results for the first few decades of the growth of relaxation times in fragile liquids are consistent with this prediction. However, the predicted divergence at T_c is not found experimentally. The value of T_c extracted from a power-law fit to data at higher temperatures is found to be substantially higher than T_g , the conventional glass transition temperature. The power law form breaks down at temperatures close to and lower than T_c , and relaxation times at T_c are typically of order 10^{-8} s. The growth of relaxation times in fragile liquids at temperatures lower than T_c is described reasonably well by the Vogel-Fulcher law¹³. Thus a temperature that is slightly higher than the T_c obtained from a power-law fit to the data at higher temperatures may be called a *crossover temperature* T_x , which separate two distinct regimes of the dynamic behavior of such liquids. These two regimes are characterized by different forms of the temperature dependence of relaxation times. A number of other experiments^{14,15} also suggest the existence of a crossover between two qualitatively different dynamical regimes at a temperature close to T_c . Recent versions of MC theories⁷⁻⁹ have established the existence of cutoff mechanisms which are supposed to round off the predicted divergence at T_c and to restore ergodicity over a much longer time scale. However, these calculations do not lead to definite predictions about the behavior to be expected at temperatures lower than T_c . It is generally believed that “activated processes” play an important role in the dynamics at these temperatures. However, the nature of these “activated processes” has not been elucidated so far.

MC theories have also been fairly successful in providing a qualitatively correct description of the decay of the time-dependent density correlation function of the supercooled liquid at temperatures higher than T_c . The decay according to this scheme takes place in a succession of several regimes: after a fast decay

in times of order of the inverse phonon frequency, a first slow decay occurs which MC theories predict to be an inverse power law in time. This is called the β -relaxation regime. Evidence for power-law decay of correlations in the β regime is provided by light and neutron scattering experiments¹⁶. According to MC theories, this decay is to a nonzero value (an apparent nonergodic phase) from which the system eventually moves away leading to the primary or α -relaxation regime. The relaxation in the α regime is found to follow the so-called Kohlrausch-Williams-Watts “stretched exponential” form¹⁷. The duration of the β relaxation and the time scale of the stretched exponential decay in the α regime are found to increase sharply as the “glass transition” is approached. In some cases, the β and the α regimes are separated by a region of so-called von Schweidler relaxation which has a power law form. The stretched exponential behavior in the α regime and the von Schweidler relaxation are seen in dielectric measurements and neutron scattering experiments¹⁶. Thus, MC theories provide a qualitative understanding of a number of experimentally observed features of glassy relaxation. However, some of the detailed MC predictions are not in agreement with experiment¹⁸ and the MC description clearly fails to account for the behavior observed at temperatures close to and lower than T_c .

In contrast to MC theories, which portray the glass transition as being purely dynamic in nature, there have been a number of attempts¹⁹⁻²² to develop a “thermodynamic” theory in which some of the interesting behavior observed near the glass transition (especially the behavior observed at temperatures lower than T_c) is attributed to an underlying continuous phase transition. These attempts have been motivated by the fact that the observed growth of the relaxation time in fragile liquids is well-described by the Vogel-Fulcher law¹³ which predicts an exponential divergence at a characteristic temperature T_0 . This temperature is found to be well below the conventional T_g . This observation suggests the possibility of a so-called “thermodynamic glass transition” that would take place at the temperature T_0 if thermodynamic equilibrium²³ could be maintained down to this temperature. Such a transition is also suggested by the observation²⁴ that the temperature at which the entropy difference between the supercooled liquid and the crystalline solid extrapolates to zero is close to T_0 . Development of a large number of glassy local minima of the free energy and slow dynamics resulting from activated transitions between these local minima are key ingredients of the thermodynamic description. Since in practice the system falls out of equilibrium at temperatures close to T_g , a direct experimental test of the existence of such a transition is not possible. Also, no calculation that explicitly demonstrates the existence of such a transition in a physically realistic system is yet available. Thus, the

“thermodynamic glass transition” scenario remains essentially speculative.

It is evident from this brief survey of the current status of the glass transition problem that a need exists for the development of new analytic and numerical methods which may address some of the outstanding issues related to this problem. In this article, we review the results^{25–27} obtained from the application of a new numerical method to a study of the dynamic behavior of a dense hard-sphere liquid near the glass transition. This method consists of direct numerical integration of a set of Langevin equations which describe the nonlinear fluctuating hydrodynamics of the system. Information about the static structure of the liquid is incorporated in the Langevin equations through a free-energy functional which has a form suggested by Ramakrishnan and Yussouff (RY)²⁸. It has been shown^{29,30} that the RY free energy functional provides a correct mean-field description of the statics of the glass transition in this system. In showing this, a numerical procedure was used to locate local minima of a discretized version of the RY free energy appropriate for the hard sphere system. A large number of glassy local minima with inhomogeneous but aperiodic density distribution were found to appear as the average density was increased above the value at which equilibrium crystallization takes place. At higher densities, the free energies of these minima were found to drop below that of the minimum representing the uniform liquid, signaling a mean-field glass transition. The success of the RY free energy functional in providing a correct description of the statics of the glass transition of the hard sphere system suggests that a good starting point for a study of the dynamics of this system would be obtained by incorporating this free energy in the appropriate NFH equations.

Several important issues are addressed in the dynamical studies reviewed here. A comparison of the results of these studies with existing molecular dynamics (MD) results^{31,32} on the same system provides a way of testing the validity of the NFH description which is cast in terms of coarse-grained number and current density variables instead of the coordinates and momenta of individual particles. The correctness of the NFH equations considered, although usually taken for granted, is not obvious in view of the fact that the hydrodynamic terms in these equations describe the physics at relatively long length scales, whereas the terms arising from the free energy functional involve length scales of the order of (or smaller than) the interparticle spacing. In the RY free energy functional, information about the microscopic interactions is incorporated in the form of the Ornstein-Zernike direct pair correlation function³³ of the liquid. This appears to be adequate for a correct description of the statics of the freezing of the liquid into both crystalline²⁸ and glassy^{29,30} states. One of the questions addressed in the work reviewed here is whether this is

also sufficient for a correct description of the dynamic behavior. Since the NFH equations considered incorporate the correct short-range structure of the dense liquid, these Langevin studies provide an opportunity to investigate in general the role of static structure in the dynamics of a dense liquid. As mentioned above, the MC equations can be derived from perturbative treatments of NFH equations which are very similar to the ones consider here. Apart from numerical errors arising from spatial discretization and the integration procedure, the numerical treatment of these NFH equations is exact. In particular, their numerical solution is obviously nonperturbative. Therefore, a comparison of the Langevin results with MC predictions provides a way to test the validity of some of the approximations made in analytic studies. Finally, by monitoring which minima of the free energy are visited during the simulated time evolution of the system, it is possible to determine whether the observed dynamic behavior arises from nonlinearities of density fluctuations in the liquid or from transitions among different glassy minima of the free energy. It is not possible to distinguish between the effects of these two kinds of processes in conventional MD simulations.

The rest of the paper is organized as follows. In Section II, we define the models considered in the work reviewed, discuss their statics and the derivation of the appropriate NFH equations, and describe the numerical method used to integrate these equations forward in time. The results obtained from the numerical work are described in detail in Section III. We also compare and contrast the results with those obtained from MD simulations of the hard-sphere and similar systems and the predictions of MC theories. Section IV contains a summary of the main conclusions drawn and a discussion of their implications for the interpretation of experimental and numerical data on the dynamics of simple supercooled liquids.

II. MODEL AND METHODS

The work that we review here is grounded in the numerical solution of a set of Langevin equations appropriate to a dense hard-sphere fluid. The statics of the model is given in terms of a free energy functional of the two fields in the problem: the number density field $\rho(\mathbf{r}, t)$ and the corresponding current density $\mathbf{g}(\mathbf{r}, t)$. This free energy has two terms:

$$F_{Tot}[\rho, \mathbf{g}] = (m_0/2) \int d\mathbf{r} \frac{|\mathbf{g}(\mathbf{r})|^2}{\rho_0} + F[\rho] \quad (2.1)$$

where m_0 is the mass of a hard sphere and ρ_0 is the average number density. In most of the work considered here $F[\rho]$ is taken to be of the RY form²⁸:

$$F[\rho] = F_l[\rho_0] + k_B T \left[\int d\mathbf{r} \{ \rho(\mathbf{r}) \ln(\rho(\mathbf{r})/\rho_0) - \delta\rho(\mathbf{r}) \} - (1/2) \int d\mathbf{r} \int d\mathbf{r}' C(|\mathbf{r} - \mathbf{r}'|) \delta\rho(\mathbf{r}) \delta\rho(\mathbf{r}') \right]. \quad (2.2)$$

In Eq.(2.2), $\delta\rho(\mathbf{r}) \equiv \rho(\mathbf{r}) - \rho_0$ is the deviation of the number density field from its average value ρ_0 , F_l is the free energy of the uniform liquid at density ρ_0 , T is the temperature, k_B is the Boltzmann constant, and $C(|\mathbf{r} - \mathbf{r}'|)$ is the Ornstein-Zernike direct pair correlation function of the uniform liquid at density ρ_0 . The inclusion of this function in the free energy ensures that upon linearization of the logarithm in the first term on the right hand side of Eq.(2.2), one obtains the usual expression for $S_s(k)$, the wavevector dependent static structure factor of a simple fluid in terms of the Fourier transform of C :

$$S_s(k) = 1/[1 - \rho_0 C(k)] \quad (2.3)$$

For hard spheres a simple expression for $C(r)$ can be obtained in the Percus-Yevick approximation³³:

$$C(\xi) = -\lambda_1 - 6\eta_f \lambda_2 \xi - (1/2)\eta_f \lambda_1 \xi^3 ; \quad \xi < 1 \quad (2.4a)$$

$$C(\xi) = 0 ; \quad \xi > 1 \quad (2.4b)$$

where $\xi \equiv r/\sigma$, η_f is the packing fraction:

$$\eta_f = (\pi/6)\rho_0\sigma^3 \equiv (\pi/6) n^* \quad (2.5)$$

and:

$$\lambda_1 = (1 + 2\eta_f)^2 / (1 - \eta_f)^4 \quad (2.6)$$

$$\lambda_2 = -(1 + \eta_f/2)^2 / (1 - \eta_f)^4. \quad (2.7)$$

In the above equations, σ is the diameter of a hard sphere. The dimensionless density n^* , which is the basic control parameter for the hard sphere system, is defined in Eq.(2.5). We have written ρ_0 in the denominator of the g^2 term in Eq.(2.1), rather than $\rho(\mathbf{r})$, so that the full density dependence of the free energy is given by the RY form. As pointed out in Ref.[34], if ρ were used, one would obtain upon functional integration with respect to g^2 a $\ln(\rho)$ contribution involving density fluctuations associated with the kinetic energy which were already included in Eq. (2.2).

In order to rewrite all equations in terms of dimensionless quantities, it is convenient to take m_0 as the unit of mass, to choose h , the lattice constant

of the computational lattice to be the unit of length, and to take the unit of time to be

$$t_0 = h/c \quad (2.8)$$

where c is the speed of sound. After the ratio h/σ is chosen as discussed below, this unit of time is²⁵ of the same order as the inverse characteristic phonon frequency and within a factor of order unity of the usual hard-sphere Enskog³⁵ collision time.

The following dimensionless quantities can then be defined:

$$\mathbf{x} = \mathbf{r}/h \quad (2.9)$$

$$n = \rho h^3 \quad (2.10)$$

$$\mathbf{j} = \mathbf{g} h^3 / c \quad (2.11)$$

and also the dimensionless free energy $F[n, \mathbf{j}]$:

$$F[n, \mathbf{j}] = (1/2) \int d\mathbf{x} \frac{|\mathbf{j}(\mathbf{x})|^2}{n_0} + F_n[n] \quad (2.12)$$

$$\begin{aligned} F_n[n] = F_{n_0}[n_0] + K & \left[\int d\mathbf{x} \{n(\mathbf{x}) \ln(n(\mathbf{x})/n_0) - \delta n(\mathbf{x})\} \right. \\ & \left. - (1/2) \int d\mathbf{x} \int d\mathbf{x}' C(|\mathbf{x} - \mathbf{x}'|) \delta n(\mathbf{x}) \delta n(\mathbf{x}') \right], \end{aligned} \quad (2.13)$$

where $K = \frac{k_B T}{m_0 c^2}$ and n_0 is the average dimensionless density. For hard spheres K depends only on the density.

The dynamics of the system is given by the Langevin equations for the set of hydrodynamic variables $\{\psi_\alpha\} \equiv \{n(\mathbf{x}, t), \mathbf{j}(\mathbf{x}, t)\}$. These equations can be written as^{8,36}:

$$\frac{\partial \psi_\alpha}{\partial t} = V_\alpha[\psi] - \sum_\beta \Gamma_{\alpha, \beta} \frac{\delta F}{\delta \psi_\beta} + \Theta_\alpha \quad (2.14)$$

where Γ is a matrix of transport coefficients, Θ are gaussian noise fields, and the V_α are the streaming velocities, which incorporate the nondissipative part of the equations of motion. After calculating the Poisson brackets explicitly one obtains²⁵:

$$\frac{\partial n(\mathbf{x}, t)}{\partial t} + (1/n_0) \nabla \cdot (\mathbf{n} \mathbf{j}) = 0 \quad (2.15)$$

and:

$$\frac{\partial j_i}{\partial t} = -n \nabla_i \frac{\delta F_n}{\delta n} - (1/n_0) \sum_j \nabla_j (j_i j_j) - (1/n_0) \sum_j j_j \nabla_i j_j + (1/n_0) \eta \nabla^2 j_i + \Theta_i \quad (2.16)$$

where η is the dimensionless bare shear viscosity when one uses the units introduced above. The combination $(\zeta + \eta/3)$, where ζ is the bare bulk viscosity, is set to zero, mainly for simplicity in generating the noise correlations. The moments of the fields $\Theta_i(\mathbf{x}, t)$ satisfy:

$$\langle \Theta_i(\mathbf{x}, t) \Theta_j(\mathbf{x}', t') \rangle = -2K\lambda \eta n_0 \delta_{i,j} \nabla^2 \delta(\mathbf{x} - \mathbf{x}') \delta(t - t'), \quad (2.17)$$

where the angular brackets denote an average over the gaussian probability distribution of the noise fields and λ is a dimensionless measure of the equilibrium fluctuations. For hard spheres,³⁷ η can be written in terms of K and the density.

An important feature of Eq.(2.16) is that the term in $\delta F_n/\delta n$ which involves the direct correlation function $C(r)$ is an integral over space with range σ . Thus, one has to solve a set of integrodifferential equations with noise terms.

The procedure followed in the work reviewed here is to numerically solve Eqns.(2.15) and (2.16) on a three dimensional cubic lattice of size N^3 . A simple Euler method is used for the time integration. The main complication is the spatial integral involving the direct correlation function $C(r)$. This is overcome by creating, in the initialization of the computer program, a table listing for each lattice site the location of all neighboring sites to be integrated over and their corresponding values of $C(r)$. Additionally, since the sphere of radius σ (which is the range of $C(r)$ in the Percus-Yevick approximation) is imbedded on a coarse discrete lattice, a finer mesh than defined on the original lattice can be used to improve the accuracy of the integration. The procedures employed to integrate the resulting set of differential equations over time and to generate the gaussian noise are described in detail in Ref. 38 and references cited there.

The primary objective of the work reviewed here is to study the dynamic correlations of the system. As discussed below, this is only possible at relatively low densities $n^* \leq 0.93$, where the system reaches equilibrium within computationally attainable times. The analysis is focused on the time dependence of the dynamic structure factor $S(\mathbf{q}, t)$. Specifically, the angular average of $S(\mathbf{q}, t)$ is analyzed. On a cubic computational lattice, it is appropriate to define q , the effective length of \mathbf{q} , as:

$$q^2 = 2(3 - \cos q_x - \cos q_y - \cos q_z), \quad (2.18)$$

and to perform angular averages of \mathbf{q} -dependent quantities by averaging over values of \mathbf{q} in the first Brillouin zone, in a spherical shell of mean radius (as given by q) corresponding to that of the vector $(\pi Q/N, 0, 0)$ and thickness π/N . The value of Q ranges from 1 to approximately $3^{1/2}N$, although only a smaller range is free of finite size effects. We will, for simplicity of notation, denote quantities averaged in this way by simply dropping the vector symbol from the wavevector argument, and often we will indicate the values of q by the “shell number” Q .

The correlation functions introduced above are spatially short ranged. It is therefore not necessary to use extremely large lattice sizes. It was found^{25,38} that $N = 15$ is adequate. The choice of the ratio σ/h which fixes the length scale for the problem, is dictated by two concerns. The first is that one wishes to be able to study the dependence of the dynamics on wavevectors in a region which is of interest from the point of view of the static structure factor $S(q) \equiv S(q, t = 0)$. Thus, the unit of length must be chosen so that the position q_{max} of the main peak in $S(q)$ falls in the middle part of the range of wavevectors within the first Brillouin zone of the computational lattice. Secondly, to retard the onset of crystallization at the higher densities studied, it is helpful to choose a value of h such that σ/h is not an integer and N is not an integral multiple of σ/h . Selecting $\sigma/h = 4.6$ clearly satisfies the second requirement. This choice also leaves q_{max} well away from the zone edge for all densities, near the $Q = 8$ shell. Most of the numerical studies reviewed here were carried out with this value of σ/h . As explained in Ref.[38], it is necessary to include the parameter λ to represent the actual fluctuations through gaussian noise. Its precise value is not crucial, since it essentially amounts to a choice of the normalization of the static fluctuations $S(q)$, but it clearly must be small since the local density variables $n(\mathbf{x}, t)$ must always be positive. The results reviewed here use $\lambda = 0.001$. All other quantities depend on n^* only.

To study the density correlations, it is necessary to store, for running times $t_0 \geq t_K$, where t_0 is the time measured from the initiation of the computation and t_K the equilibration time for the current correlations²⁵, the products of the form $\delta n(\mathbf{x}, t_0)\delta n(\mathbf{x}', t_0 + t)$ for all \mathbf{x}, \mathbf{x}' . This must be done at a sufficiently large number of time bins. One then monitors the spherically averaged spatial Fourier transform, $S(q, t, t_0)$ of the quantity:

$$S(\mathbf{x}, \mathbf{x}', t, t_0) = \langle \delta n(\mathbf{x}, t_0)\delta n(\mathbf{x}', t_0 + t) \rangle \quad (2.19)$$

where the average is understood to be over a number n_b of time bins separated by an interval Δt . The time range covered by the averaging process is $t_R = n_b\Delta t$. In order for $S(q, t, t_0)$ to be an adequate approximation to the thermodynamic average $S(q, t)$, this quantity must be not only independent

of t_0 , but also independent of t_R within statistical error. Dependence on t_0 indicates the presence of a transient. Dependence on t_R indicates that the averaging time is too short for ergodicity to hold. A very important point is that the minimum value of the transient time for density fluctuations is not t_K , but it is²⁵ of the order of the slowest characteristic decay time τ^* in the system. As discussed in the next Section, τ^* is a strongly increasing function of density, and is much longer than the equilibration time for the kinetic energy. Similarly, it is necessary for the average to include a range t_R of order of several times τ^* . It turns out²⁵ that $S(q, t, t_0)$ at higher densities has considerable oscillations over t_R time ranges smaller than τ^* . Due to these reasons, the obtention of statistically reliable results for the correlation functions requires averaging over a large number of time bins. This amounts^{25,38} to averaging over an “effective number of runs”.

The above methodology is used at densities $n^* \leq 0.93$. As the density is increased beyond this value, the behavior of the system undergoes a qualitative change. Instead of locally equilibrating after a more or less brief transient, the system does not seem to reach a steady state in the time scale of the computation. Instead, the mean field free energy keeps slowly drifting. By further increasing n^* it is found²⁷ that the drift is to a value below that of the liquid minimum. The quantity

$$\delta F \equiv F_n[n] - F_{l_n}[n_0] \quad (2.20)$$

becomes negative. If one attempts to carry on with the numerical computation, very large density fluctuations begin to occur, which are characteristic of the incipient formation of a solid. It is then impossible to follow the further evolution of the system to equilibration: for one thing the time scales involved are simply too long, and furthermore, the large scale fluctuations lead to numerical instabilities. Physically, we may say that a liquid-like formalism is no longer adequate.

A different strategy²⁷ is then needed. One again integrates the dynamical equations (2.15) and (2.16). As a function of time, the equal time current correlations, the maximum value of the density field, and δF , as defined in (2.20) are then monitored. After an initial transient t_K the current correlations settle again to their equipartition theorem value. The maximum density and δF vary very slowly. The former increases with time, while the latter which at time of order t_K is small and positive, drifts downwards. Eventually these trends accelerate, the maximum value of $n(x)$ sharply increases, and δF crosses zero. In Ref.[27] we defined the time τ' (which will be discussed in the next Section) as the value of t at which this crossover occurs. For $t > \tau'$, δF becomes more negative, and the fluctuation phenomena described above become more

pronounced. A reliable value of τ' can be obtained by averaging over several runs, this time in the ordinary sense of the word: each run being a computation carried out from random initial conditions.

III. NUMERICAL RESULTS

The numerical calculation outlined in the preceding Section was carried out for several values of the dimensionless density n^* in the range $0.75 \leq n^* \leq 1.10$. As stated above, the system could be equilibrated in the liquid state during computationally accessible time scales for values of $n^* \leq 0.93$. It was found in Ref.[29] that a hard sphere system described by a discretized version of the RY free energy exhibits a crystallization transition near $n^* = 0.83$. Since the Langevin simulations described above use the same discretized free energy as that of Ref.[29], the system may be considered to be in the “supercooled” regime for a large part of the density range in which equilibrium results could be obtained. Equilibration was tested by comparing the numerical result for the static structure factor $S(q)$ with the expected one, Eq.(2.3). Good agreement between the calculated $S(q)$ and the expected $S_s(q)$ was found²⁵ for all values of n^* satisfying $n^* \leq 0.93$. We turn first to a discussion of the equilibrium dynamic correlation functions observed in this regime. As in Ref.[25] we present the results in terms of the normalized correlation function $C(q, t)$ defined as:

$$C(q, t) = \frac{S(q, t)}{S(q, t = 0)} \quad (3.1)$$

where we are dealing with angularly averaged quantities as explained above with q defined in (2.18).

In analyzing the correlation results for hard spheres, previous results obtained from simpler models can be used as a guide. Specifically, we recall the results^{34,38} obtained by the same Langevin method with simpler forms of the free energy. The model studied in Ref.[38] can be described for our purposes here as being similar to the hard sphere model of Eqs. (2.1),(2.2) but with a much simpler static structure. We refer the reader to the original work for the technical details. The linearized static structure factor $S_s(q)$ for that model is given by:

$$S_s(q) \propto 1/[1 + a(q^2 - q_0^2)^2] \quad (3.2)$$

where a and q_0 are constants. This expression should be contrasted with Eq.(2.3). This model, which contains the simplest possible “one peak” structure in its statics, has been studied theoretically by MC methods^{8,9}. The

correspondence between the parameters in this model and a hard sphere system is a somewhat intricate question³⁸. However, we can say that a qualitative change in the dynamic behavior was found as the density was increased: at lower densities the decay of $C(q, t)$ in time was simply exponential, while at higher densities it became a stretched exponential at wavevectors larger than q_0 . At the highest densities and largest wavevectors studied, evidence for a power law decay regime was also seen. Nonexponential decay at short wavelengths had already been found in a structureless model³⁴.

In the hard sphere system described in the previous Section, one begins by attempting to characterize the decay of $C(q, t)$ with a single characteristic time by fitting the data to a stretched exponential form:

$$C(q, t) = e^{-(t/\tau)^\beta} \quad (3.3)$$

where the parameters β and τ are functions of n^* and q . At fixed density within the range $n^* \leq 0.93$ where this study is possible, τ is a strong function of q having a sharp maximum at the value of q where the static structure factor²⁵ $S(q)$ has its first and most prominent peak. We identify this maximum value of τ , $\tau^*(n^*)$, with the slowest decay rate in the system. It is possible to fit this quantity to a Vogel-Fulcher¹³ law:

$$\tau^*(n^*) = \alpha e^{\gamma/(v - v_c)} \quad (3.4)$$

where $v \equiv 1/n^*$. The fit to the data obtained in Ref.[25] is shown in Fig. 1. The value of v_c in the fit corresponds to $n_c^* = 1.23$, in very good agreement with the MD result, $n_c^* = 1.21$ obtained in Ref.[31]. Although a three parameter fit of the same data to a power law is also adequate, it was found that the form (3.4) is better. Despite the fact that the time τ^* is peaked, as a function of q , at the same value q_{max} as $S(q)$ the simple form $\tau^*(q) \propto \eta S(q)$ is not obeyed. This indicates the existence of strong renormalization effects in the transport properties near glass formation, which is not surprising.

The stretched exponential form (3.3) is not always a satisfactory fit to the data for $C(q, t)$. At larger values of q it begins to be inadequate at densities as low as $n^* \approx 0.75$, while when $n^* \geq 0.90$ it fails over a wide range of wavevectors, including the peak value ($Q = 8$ in the notation introduced earlier). It was found that a general form that fits the data for $C(q, t)$ at all densities $n^* \leq 0.93$ is:

$$C(q, t) = (1 - f)e^{-(t/\tau_1)^\beta} + f e^{-t/\tau_2} \quad (3.5)$$

The form (3.5) reduces to (3.3) when $f = 0$ or alternatively, when $\tau_1 \approx \tau_2$ and $\beta \approx 1$. It can also represent quasinonergodic behavior (decay to a constant)

whenever $\tau_2 \rightarrow \infty$, which means in practice a value of τ_2 larger than the longest time computationally considered. This behavior was found²⁵ at larger wavevectors at $n^* = 0.93$, for example.

In Fig. 2 and Fig. 3 we show a selection of data from Ref.[25] and fits of the form (3.5), at densities $n^* = 0.90$ and $n^* = 0.93$, and several wavevectors. In these figures the solid curves are the fits and the dashed curves the corresponding numerical data. The case $Q = 6$ (Q is defined in the paragraph below Eq.(2.18)) corresponds, for the densities shown, to the situation where (3.3) yields a good fit to the data, with $\beta \approx 0.86$. For $Q = 10$ the decays shown are unstretched exponentials. In all other cases shown the full form (3.5) is required, with values of f ranging up to $f \approx 0.5$ at $Q = 13$. The parameter f depends strongly on q and weakly on the density. All characteristic times, on the other hand, depend strongly on both n^* and q .

We believe that these results in the two-decay regime of the full Eq. (3.5) should be interpreted as representing first the merged effects of phonon and β relaxation, leading eventually in most cases to the second decay, which we then identify with α relaxation. Thus, the data is consistent with the widely believed scenario^{3,18} of successive relaxation regimes: first a fast decay at time scales of order of the phonon time, (unity in the case discussed here) followed by β relaxation to a nonergodic phase, from which the system decays again through the von Schweidler and α (primary) relaxation regimes. The first two of these different relaxation regimes seem to have been compressed and merged together in the Langevin dynamics of the hard sphere liquid. As mentioned above, the numerical results do not show a distinct β -relaxation regime with a power-law decay of correlations: At all densities and wavevectors, the first part of the decay of $C(q, t)$ is better fit by a stretched exponential (as indicated in (3.5)) than by a power law.

As mentioned above, the characteristic time τ^* obtained from the Langevin method is in good agreement with MD results.³¹ One can also try to compare the Langevin results for the dynamic correlation functions with MD work. The comparison is obscured by the fact that in MD work glassy behavior has been discussed in terms of soft sphere mixtures^{39,40} or Coulomb systems⁴¹. The results of Ref.[39] correspond to a shorter time scale, while those of Refs.[40] and [41] do not follow $C(q, t)$ for long enough times to see it decay to a small value. These authors also assume that their system has equilibrated when the kinetic energy reaches its equipartition theorem equilibrium value. For the Langevin system, this assumption was found²⁵ to be erroneous. While these caveats should be kept in mind, it is nevertheless true that the Langevin and MD results seem fully compatible. The main difference is the absence in the Langevin case of any sharp feature in the phonon scale. This absence should

be attributed to Langevin coarse graining of the time scale, or perhaps, to poor equilibration in the MD work. Otherwise the Langevin results are consistent with MD in the sense that the form (3.5) with well separated time scales and relatively large f provides a good description of the MD plots.

We turn now to the results for higher densities²⁷. We have earlier explained how the correlation functions cannot be evaluated for $n^* > 0.93$. One can then use the strategy described in the last Section to evaluate the characteristic time τ' defined as the time at which δF (see Eq. (2.20)) vanishes.

The values of τ' were obtained in this fashion in Ref. [27]. They were found to vary from run to run but only slightly. The average value as a function of density is plotted in Fig. 4. The results for τ' from the fit 3.4 are also shown for comparison. One clearly sees that τ' decreases very sharply with increasing density, until it becomes approximately independent of n^* beyond $n^* \approx 1$.

Since τ^* , on the other hand, increases with density, the curves for τ^* and τ' cross, at a density $n^* \approx 0.98$. The main feature of the observed dependence of τ' on the density is the sharp change in τ' which takes place as the density approaches a *crossover* value $n_x^* \approx 0.95$.

The evolution of the system beyond time τ' can be inferred in the following way²⁷: The final state configuration at time τ' , as obtained from the dynamical simulation, is used as the input in a minimization routine that finds the free-energy minimum lying closest in phase space to the initial configuration. The nature of the distribution of the local density at this free-energy minimum can then be examined. The minimization routine, then, acts as a surrogate fast dynamics to quickly determine the nature of the configuration the system would slowly evolve to. If the minimization procedure is applied to configurations obtained when δF is still positive, the flow is invariably found to be to the uniform liquid minimum. In contrast, the minima to which configurations obtained after δF has become negative converge correspond to highly inhomogeneous distributions, with the density concentrated at only a few points.

There are several quantities which characterize the nature of the density distribution at these minima. One of these quantities is a two-point density correlation function $u(r)$. The function $u(r)$ for a particular minimum reached by the system, characterized by the values $\{n_i\}$ of the dimensionless density variables at the computational lattice points $\{i\}$, is defined as:

$$u(r) = \frac{1}{(n_{av})^2} \frac{\sum_{i>j} n_i n_j f_{ij}}{\sum_{i>j} f_{ij}}, \quad (3.6)$$

where n_{av} is the average value of n_i and $f_{ij}(r) = 1$ if the separation between the mesh points i and j of the computational lattice lies between r and $r + \Delta r$, and $f_{ij} = 0$, otherwise. This function describes spatial correlations of the time-

averaged local density at a local minimum of the free energy. It is different from the more familiar pair distribution function $g(r)$ which describes equal-time correlations of the instantaneous local density. The function $u(r)$ is equal to unity for all r in the uniform liquid minimum. In an inhomogeneous minimum it is not strictly equal to zero for all $r < \sigma$ because the average density near a point where a particle is localized in such a minimum is smeared out over a region of width $\approx 0.3\sigma$. The results for $u(r)$ obtained in Ref[27] do not correspond to a liquid. The r -dependence of $u(r)$ for $r \leq 2.5\sigma$ (information about larger distances is less reliable due to sample size effects) looks very similar to that of the pair-distribution function of the “slowly quenched” glassy states found in MD simulations³² of the hard sphere system. There appear to be significant differences between the form of $u(r)$ and that of the pair-distribution function $g(r)$ of the imperfect crystalline state obtained via nucleation from the liquid state in MD simulations³². In particular, $g(r)$ of the nucleated crystal exhibits a pronounced peak at $r \approx 1.6\sigma$, which is just barely present in the data for $u(r)$. The heights of the secondary peaks of $u(r)$ (which are near $r \approx 1.9\sigma$ and $r \approx 2.3\sigma$) are smaller than the heights of the corresponding peaks of $g(r)$ for the nucleated crystalline state. These discrepancies may be due to differences in sample size, boundary conditions etc., and in the absence of reliable data on the form of $u(r)$ for larger values of r , it is difficult to decide from this information alone whether the inhomogeneous minima obtained in Ref.[27] are glassy or crystalline with defects.

The nature of the local arrangement of the particles can be further investigated through evaluation of the bond-orientational “order parameters”, Q_l and W_l , introduced by Steinhardt *et al*⁴². These quantities are defined as follows: The mesh points at which the density is peaked in an inhomogeneous minimum of the free energy represent the locations of the hard-sphere particles. Two such particles are considered to be neighbors if the separation between the corresponding mesh points is less than 1.4σ , the approximate value of r at the first minimum of $u(r)$. Let \mathbf{R}_i denote the location of such a particle and let $\theta^\alpha(\mathbf{R}_i)$ and $\phi^\alpha(\mathbf{R}_i)$ be the polar and azimuthal angles which specify the orientation of a unit vector pointing from this particle to its α th neighbor. Following Ref.[43], one defines the quantity $Q_{lm}(\mathbf{R}_i)$ for this particle as

$$Q_{lm}(\mathbf{R}_i) \equiv \frac{1}{m_l} \sum_{\alpha} Y_{lm}(\theta^\alpha(\mathbf{R}_i), \phi^\alpha(\mathbf{R}_i)), \quad (3.7)$$

where m_l is the number of neighbors of this particle and $Y_{lm}(\theta, \phi)$ is a spherical harmonic. The “order parameters” $Q_l(\mathbf{R}_i)$ and $W_l(\mathbf{R}_i)$ are defined as rotationally invariant combinations of the $Q_{lm}(\mathbf{R}_i)$:

$$Q_l(\mathbf{R}_i) \equiv \left(\frac{4\pi}{2l+1} \sum_{m=-l}^l |Q_{lm}(\mathbf{R}_i)|^2 \right)^{1/2}, \quad (3.8)$$

and

$$W_l(\mathbf{R}_i) \equiv \frac{1}{(\sum_m |Q_{lm}(\mathbf{R}_i)|^2)^{3/2}} \sum_{m_1, m_2, m_3} \begin{pmatrix} l & l & l \\ m_1 & m_2 & m_3 \end{pmatrix} \times \delta_{m_1+m_2+m_3,0} Q_{lm_1}(\mathbf{R}_i) Q_{lm_2}(\mathbf{R}_i) Q_{lm_3}(\mathbf{R}_i), \quad (3.9)$$

where $\begin{pmatrix} l & l & l \\ m_1 & m_2 & m_3 \end{pmatrix}$ is a Wigner $3j$ symbol. The values of $Q_l(\mathbf{R}_i)$ and

$W_l(\mathbf{R}_i)$ for $l = 4$ and 6 provide^{42,43} useful information about the symmetry of the local arrangement of particles surrounding the one at \mathbf{R}_i . For example, the values of Q_4 , Q_6 , W_4 and W_6 are $(0.19, 0.57, -0.16, -0.013)$, $(0.036, 0.51, 0.16, 0.013)$, $(0.097, 0.48, 0.13, -0.012)$ and $(0, 0.66, 0, -0.17)$ for fcc, bcc, hcp and icosahedral clusters, respectively. The results for Q_4 and Q_6 , obtained for the inhomogeneous local minima found in Ref.[27], are consistent with local fcc order: The distribution of $Q_4(\mathbf{R}_i)$ peaks near 0.21, which is also the average value of $Q_4(\mathbf{R}_i)$. This value is close to what is expected for a cluster with fcc symmetry. The distribution of $Q_6(\mathbf{R}_i)$ peaks near 0.43 and its average value is close to 0.46. Since all close-packed structures (fcc,bcc,hcp and icosahedral) have large values of Q_6 , it is not possible to draw any conclusion about the nature of the local bond-orientational order from this observation. The distribution of W_4 shows significant weight in the region near -0.14 , close to the value (-0.16) expected for a fcc cluster. However, the distribution is fairly wide and the average value of W_4 (≈ -0.026) is rather different from the fcc value. The distribution of $W_6(\mathbf{R}_i)$ exhibits a peak in the neighborhood of the value (-0.013) expected for a fcc cluster, but has significant weight at negative values with a larger magnitude, indicating the presence of a substantial amount of local icosahedral order which is expected⁴² in a random close-packed arrangement of hard spheres. The observed distribution of W_6 is consistent with similar data obtained in MD simulations⁴³ of glassy states of a Lennard-Jones system.

To summarize, the nature of the arrangement of the local density in the inhomogeneous minima reached by the system (at larger values of n^*) after it makes a transition away from the uniform liquid minimum shows that these minima exhibit a number of features characteristic of a fcc solid. At the same time, some of the features expected for a random close-packed structure also

appear to be present. Of course, there is no meaningful difference between the short-range correlations of a glass and those in a very disordered crystal, so that the question of whether a finite-size system is glassy or a very defective crystal is not really well-posed.

The observation that the system makes a transition away from the uniform liquid minimum of the free energy within computationally accessible time scales if the density exceeds a certain crossover value n_x^* is in qualitative agreement with results obtained from MD simulations³² of the hard sphere liquid. These simulations show that the hard sphere system cannot be locally equilibrated in the supercooled liquid state if the density n^* exceeds a “critical value” $n_s^* \simeq 1.08$. If the liquid is allowed to evolve in time at a density equal to or higher than n_s^* , then it spontaneously freezes into an imperfect fcc solid during the time scale of the simulation. If, on the other hand, the system is rapidly compressed from the liquid state at a density lower than n_s^* to a density close to the random close packing density ($n^* \simeq 1.23$), then it ends up in an amorphous state. The degree of “glassiness” of this amorphous state increases with the rapidity of the process of compression. These results look similar to the behavior observed in the Langevin numerical results if we identify the crossover density n_x^* obtained from these computations with the critical density n_s^* found in the MD simulation. The value of n_x^* obtained from our simulation ($n_x^* \simeq 0.95$) is somewhat different from the result ($n_s^* \simeq 1.08$) of MD simulations. This difference probably arises from the fact that the value of n^* at which the discretized version of the RY free energy functional used in Refs.[25–27] exhibits a thermodynamic crystallization transition ($n_f^* \simeq 0.83$)^{29,30} is substantially lower than the crystallization density obtained in MD simulations ($n_f^* \simeq 0.943$)³². The value of the ratio, $n_x^*/n_f^* \simeq 1.14$, obtained²⁷ in the Langevin equation work is quite close to the value of n_s^*/n_f^* ($\simeq 1.15$) obtained in the MD simulation.

IV. DISCUSSION

We first summarize the main results obtained from the work reviewed here. For hard spheres the density, rather than the temperature, is the control parameter. The effect of increasing (decreasing) the density is analogous to that of decreasing (increasing) the temperature of systems for which the usual control parameter is the temperature. In the Langevin method computational results described above, it was found that the system can be locally equilibrated in the metastable “supercooled” liquid state during computationally accessible time scales as long as the density is relatively low ($n^* \leq 0.93$). The

dynamic behavior observed in this regime exhibits a number of characteristic glassy features. These include stretched exponential decay of correlations, two-stage relaxation, and Vogel-Fulcher growth of relaxation times. The observed behavior is in quantitative agreement with existing MD data on the dynamics of the hard-sphere liquid and in qualitative agreement with other MD results obtained for similar systems. These observations help establish the correctness of the NFH description used in this work and also demonstrate that the RY free energy contains the essential physics of the dynamics of this system. These calculations also reproduce qualitatively a number of predictions of MC theories. Another important observation is that the onset of glassy features in the decay of $S(q, t)$ occurs at relatively lower densities for wavevectors close to the first and second peaks in the static structure factor. This result clearly illustrates the important role played by the equilibrium structure in the long-time dynamics of the liquid. The observed q -dependence of the decay of $S(q, t)$ also suggests that the glassy behavior sets in earlier (at lower densities) at shorter length scales. Finally, the system is found to fluctuate about the liquid-state minimum of the mean field free energy in the density range studied. This implies that all the glassy features found in this regime arise from nonlinear interactions of small-amplitude density fluctuations about the uniform liquid minimum of the free energy. The qualitative agreement between the Langevin method results and the predictions of MC theories suggests that these theories provide an adequate description of the physics of these nonlinear interactions.

The numerical results at higher densities reveal the existence of a new time scale $\tau'(n^*)$, which corresponds to the amount of time a system, initially prepared in a state close to the uniform liquid minimum of the free energy, spends in the vicinity of this minimum before making a transition to one of the many inhomogeneous local minima of the free energy. This time scale is found to decrease sharply as the dimensionless density n^* is increased above a characteristic value, $n_x^* \simeq 0.95$, and it exceeds the time scales accessible in numerical work for lower values of n^* . The free-energy minima to which the system makes transitions for $n^* > n_x^*$ are highly inhomogeneous, representing either crystalline states with many defects or glassy states. Comparison with existing MD data suggests that these states should be identified as near-crystalline ones. The fact that in simulations carried out at densities equal to or greater than n_x^* , the liquid is able to freeze into a state which is close to the crystalline one indicates that the free-energy minima which represent near-crystalline states must be fairly easy to reach. Otherwise, the system would not be able to bypass the large number of glassy minima which are known^{29,30} to be present at such densities. There are other simple model systems (such as the Lennard-Jones liquid and the one-component plasma) which, according

to MD results, exhibit nucleation⁴⁴ of the crystalline phase at sufficiently high degrees of supercooling. This observation suggests that a similar picture holds for these models too.

The observations summarized above suggest the following scenario for the dynamics of such simple liquids in the supercooled regime. For densities lower than the crossover density n_x^* (alternatively, for temperatures higher than a crossover temperature T_x when the temperature T is the control parameter), the system remains in the vicinity of the uniform liquid minimum during the time scale of observation. The dynamics in this regime is, therefore, governed by small fluctuations about the liquid minimum. Nonlinear interactions of these density fluctuations lead to a growth of the relaxation time as the density is increased (temperature is decreased). As noted above, MC theories are expected to provide a good description of the non-linear feedback mechanism that causes this growth of the relaxation time. Therefore, the dynamic behavior of the system in this regime would be well-described by MC theories. As the density is increased above n_x^* (the temperature is decreased below T_x), the system undergoes a transition from the liquid minimum to a near-crystalline one within the time scale of observation and remains in its vicinity for all later times. Typically, the value of $n_x^*(T_x)$ is found to be lower (higher) than that of $n_c^*(T_c)$ extracted from power-law fits to the data at lower densities (higher temperatures). For example, the value of n_x^* obtained from MD simulations³² of the hard sphere liquid is close to 1.08, whereas power-law fits to the MD data³¹ for the diffusion constant¹² and the relaxation time data obtained in the work^{25,26} reviewed here yield values of n_c^* in the range 1.10 – 1.15. Thus, questions about a crossover in the dynamic behavior of the supercooled liquid near $n_c^*(T_c)$ do not arise in these systems and the dynamics over the entire accessible supercooled regime is well-described by MC theories. All existing simulation data, including our own, on these systems are consistent with this scenario.

There are, however, many systems for which this simple picture is not applicable. Many model systems, such as two-component mixtures with spherically symmetric interactions^{39,40,45}, do not show any sign of crystallization during the time scale of MD simulations. There are also a large number of experimentally studied systems (so-called good glass-forming liquids¹⁶) which can be maintained in the liquid state for long times at high degrees of supercooling without the occurrence of crystallization. The results of the simulations reviewed here suggest the following picture of the dynamics of such systems in the supercooled liquid regime.

As T is lowered below the equilibrium freezing temperature T_f , the appropriate free-energy functional describing the system is expected to develop

a large number of inhomogeneous local minima. Some of these minima have crystalline or near-crystalline structures and the others are amorphous. At temperatures well below T_f , all of these minima have free energies lower than that of the uniform liquid minimum. The conventional mean-field description of metastability suggests that the typical height (V) of the free-energy barriers which separate the liquid minimum from these inhomogeneous minima should decrease as the temperature is lowered. This, however, does not necessarily mean that the typical time scale for transitions away from the liquid minimum also decreases with temperature. This time scale is expected to be proportional to $e^{V/T}$, which may increase as T is decreased even if V decreases with decreasing T . Thus, it is not easy to predict whether the time scale τ' ever becomes experimentally accessible in such a system. However, we note that there exist a large amount of experimental data (summarized in Ref. 2) which indicate that the dynamics of the liquid at temperatures close to and lower than T_c is dominated by processes associated with the exploration of a large part of the full phase space (excluding the regions near the equilibrium crystalline states). These observations suggest that the time scale τ' in these systems becomes comparable to typical experimental time scales at a temperature T_x which is higher than T_c . If this is so, then the following situation can be expected for the dynamics of the system in the supercooled regions. For temperatures higher than T_x , a system initially prepared in the liquid state remains in the vicinity of the liquid minimum for long times and its dynamic behavior is well-described by MC theories. Since temperatures higher than T_x are substantially higher than T_c , the temperature dependence of the relaxation time in this regime would follow the power-law form predicted in the original version of MC theories. We believe that all temperatures at which a liquid can be equilibrated within the time scale accessible in MD simulations lie in this regime. This would explain the observed agreement between the results obtained from MD simulations³⁹⁻⁴¹ and the predictions of MC theories. The growth of relaxation times in this regime is a purely kinetic phenomenon, not related to or caused by the growth of any spatial correlation. This is consistent with two recent numerical studies^{45,46} which looked for a growing correlation length in this regime and did not find any evidence for its existence.

The dynamic behavior for temperatures lower than T_x would be qualitatively different. At these temperatures, the system would make a transition from the liquid minimum to one of the inhomogeneous minima of the free energy during the time scale of observation. In good glass-forming liquids, these inhomogeneous minima are more likely to be glassy than crystalline. Since these free-energy minima are expected to have lower free energies than that of the uniform liquid minimum at temperatures lower than T_x , the liquid mini-

mum would not play any significant role in the dynamics at later times. To understand the nature of the dynamics in this regime, it is necessary to have estimates of the heights of free energy barriers which separate different glassy minima. Unfortunately, reliable information about the distribution of these barrier heights is not available. Approximate calculations⁴⁷ and the experimental observation that the system behaves like a liquid over a substantial range of temperatures below T_c suggest that these barrier heights remain finite in the thermodynamic limit at these temperatures. If this is so, then the system would visit many such minima during its evolution over a long time. It would, therefore, behave like a liquid over such time scales, in the sense that the time-averaged local density would be uniform. However, the dynamics of the system would be very different in this regime because the decay of density fluctuations would be determined primarily by activated transitions among various glassy local minima of the free energy. Thus, the presence of a crossover in the dynamic behavior of the system near a temperature T_x which is higher than the temperature T_c obtained from power-law fits to the data obtained at higher temperatures would follow naturally from these considerations.

If the picture described above is correct, then the dynamics of such systems at temperatures lower than T_x would have many similarities with that of quenched random systems such as spin glasses which are known⁴⁸ to exhibit a large number of local minima of the free energy at low temperatures. In particular, the suggestion^{19,20,22} that a true thermodynamic phase transition would take place at a lower temperature T_g if thermodynamic equilibrium could be maintained all the way down to this temperature would become a distinct possibility. It is interesting to note in this context that the results obtained from a recent experiment¹⁵ have been interpreted as evidence for the existence of a length scale that grows as the temperature is lowered below T_c .

In the absence of any direct corroborative evidence, this description of the dynamics of good glass-forming liquids in the supercooled region remains essentially speculative. It would be very interesting to look for evidence for or against this scenario in experiments and simulations.

ACKNOWLEDGMENTS

One of us (C. D.) thanks the University of Minnesota Physics Department for hospitality. We thank L.M. Lust for help with part of the original work reviewed here and S. Ramaswamy and G. Mazenko for discussions.

REFERENCES

- ¹ J. Jäckle, Rep. Prog. Phys. **49**, 171, (1986).
- ² C. A. Angell, J. Phys. Chem. Solids, **49**, 863, (1988).
- ³ For reviews of mode coupling theories, see B. Kim and G. F. Mazenko, Adv. Chem. Phys. **78**, 129 (1990); W. Götze in *Liquids, Freezing and the Glass Transition*, eds D. Levesque, J. P. Hansen and J. Zinn-Justin (Elsevier, New York, 1991).
- ⁴ E. Leutheusser, Phys. Rev. A **29**, 863 (1984).
- ⁵ U. Bengtzelius, W. Götze and A. Sjolander, J. Phys. C **17**, 5915 (1984).
- ⁶ W. Götze, Z. Phys. **60**, 195, (1985).
- ⁷ W. Götze and L. Sjogren, Z. Phys. B **65**, 415 (1987); J. Phys. C **21**, 3407 (1988); J. Phys. Cond. Matt. **1**, 4183 (1989).
- ⁸ S. P. Das and G. F. Mazenko, Phys. Rev. A **34**, 2265 (1986).
- ⁹ S. P. Das, Phys. Rev. A **36**, 211 (1987).
- ¹⁰ For a review of the NFH formalism, see B. Kim and G. F. Mazenko, J. Stat. Phys. **64**, 631 (1991).
- ¹¹ T. R. Kirkpatrick, Phys. Rev. A **31**, 939, (1985).
- ¹² J. L. Barrat, W. Götze and A. Latz, J. Phys. Condens. Matt. **1**, 7163 (1989).
- ¹³ H. Vogel, Z. Phys. **22**, 645, (1921); G. S. Fulcher, J. Amer. Ceram. Soc. **8**, 339, (1925).
- ¹⁴ E. Rössler, Phys. Rev. Lett. **65**, 1595 (1990).
- ¹⁵ E. W. Fisher, E. Donth and W. Stephen, Phys. Rev. Lett. **68**, 2344 (1992).
- ¹⁶ For a review of recent experiments with comparisons to predictions of MC theories, see *Dynamics of Disordered Materials*, edited by D. Richter, A. J. Dianoux, W. Petry and J. Teixeira (Springer, Berlin, 1989).
- ¹⁷ G. Williams and D. C. Watts, Trans. Faraday Soc. **66**, 80 (1970).
- ¹⁸ B. Kim and G. F. Mazenko, Phys. Rev. A **45**, 2393, (1992).
- ¹⁹ D. L. Stein and R. G. Palmer, Phys. Rev. B **38**, 12035 (1988).
- ²⁰ T. R. Kirkpatrick, D. Thirumalai and P. G. Wolynes, Phys. Rev. A **40**, 2 (1989).

²¹ J. P. Sethna, *Europhys. Lett.* **6**, 529 (1989).

²² J. P. Sethna, J. D. Shore and M. Huang, *Phys. Rev. B* **44**, 4943 (1991).

²³ Here, and elsewhere in the paper, the term “thermodynamic equilibrium” means equilibrium over a restricted phase space that excludes the crystalline state .

²⁴ W. Kauzmann, *Chem. Rev.* **48**, 219 (1948).

²⁵ L.M. Lust, O.T. Valls, and C. Dasgupta, *Phys. Rev. E* **48**, 1787, (1993).

²⁶ L. M. Lust, O. T. Valls and C. Dasgupta, *Phase Transitions* **50**, 47 (1994).

²⁷ C. Dasgupta and O.T. Valls, *Phys. Rev. E* **50**, in press.

²⁸ T.V. Ramakrishnan and M Yussouff, *Phys. Rev. B* **19**, 2275, (1979).

²⁹ C. Dasgupta, *Europhys. Lett.* **20**, 131 (1992).

³⁰ C. Dasgupta and S. Ramaswamy, *Physica A* **186**, 314 (1992).

³¹ L.V. Woodcock and C.A. Angell, *Phys. Rev. Lett.* **47**, 1129, (1981).

³² L.V. Woodcock, *Ann. N.Y. Acad. Sci.* **371**, 274, (1981).

³³ See J.P. Hansen and I.R. MacDonald, *Theory of simple liquids* (Academic, London, 1986).

³⁴ O.T. Valls and G.F. Mazenko, *Phys. Rev. A* **44**, 2596, (1991).

³⁵ W.E. Alley, B.J. Alder, and S. Yip, *Phys. Rev. A* **27**, 3174, (1981).

³⁶ J.E. Farrell and O.T. Valls, *Phys. Rev. A* **40**, 7027, (1989).

³⁷ J.P. Boon and S. Yip, *Molecular Hydrodynamics*, (Mc Graw- Hill, N.Y. 1990), Eq. 2.4.40.

³⁸ O.T. Valls and G.F. Mazenko, *Phys. Rev. A* **46**, 7756 (1992).

³⁹ J.J. Ullo and S. Yip, *Chem. Phys.* **149**, 221, (1990).

⁴⁰ J.-L. Barrat, J.-N. Roux and J.-P. Hansen, *Chem. Phys.* **149**, 197 (1990).

⁴¹ G.F. Signorini, J.-L. Barrat, and M.W. Klein, *J. Chem. Phys.* **92**, 197 (1990).

⁴² P.J. Steinhardt, D.R. Nelson, and M. Ronchetti, *Phys. Rev. B* **28**, 784, (1983).

⁴³ S. Nosé and F. Yonezawa, *J. Chem. Phys.* **84**, 1803, (1986). See also F. Yonezawa in *Solid State Physics*, v. 45, ed. by H. Ehrenreich and D. Turnbull, (Academic Press, Boston, 1991).

⁴⁴ For a review of homogeneous nucleation, see D. Frenkel and J. P. McTague, *Annu. Rev. Phys. Chem.* **31**, 491 (1980); K. F. Kelton in *Solid State Physics*, edited by H. Ehrenreich and D. Turnbull (Academic Press, Boston, 1991),

⁴⁵ C. Dasgupta, A. V. Indrani, S. Ramaswamy and M. K. Phani, *Europhys. Lett.* **15**, 307 (1991).

⁴⁶ R. M. Ernst, S. R. Nagel and G. S. Grest, *Phys. Rev. B* **43**, 8070 (1991).

⁴⁷ R. W. Hall and P. G. Wolynes, *J. Chem. Phys.* **86**, 2943 (1987); P. G. Wolynes in *Proceedings of International Symposium on Frontiers in Science, (AIP Conf. Proc. No. 180)*, eds. S. S. Chen and P. G. Debrunner (AIP, New York, 1988).

⁴⁸ See, for example, K. Binder and A. P. Young, *Rev. Mod. Phys.* **58**, 881 (1986).

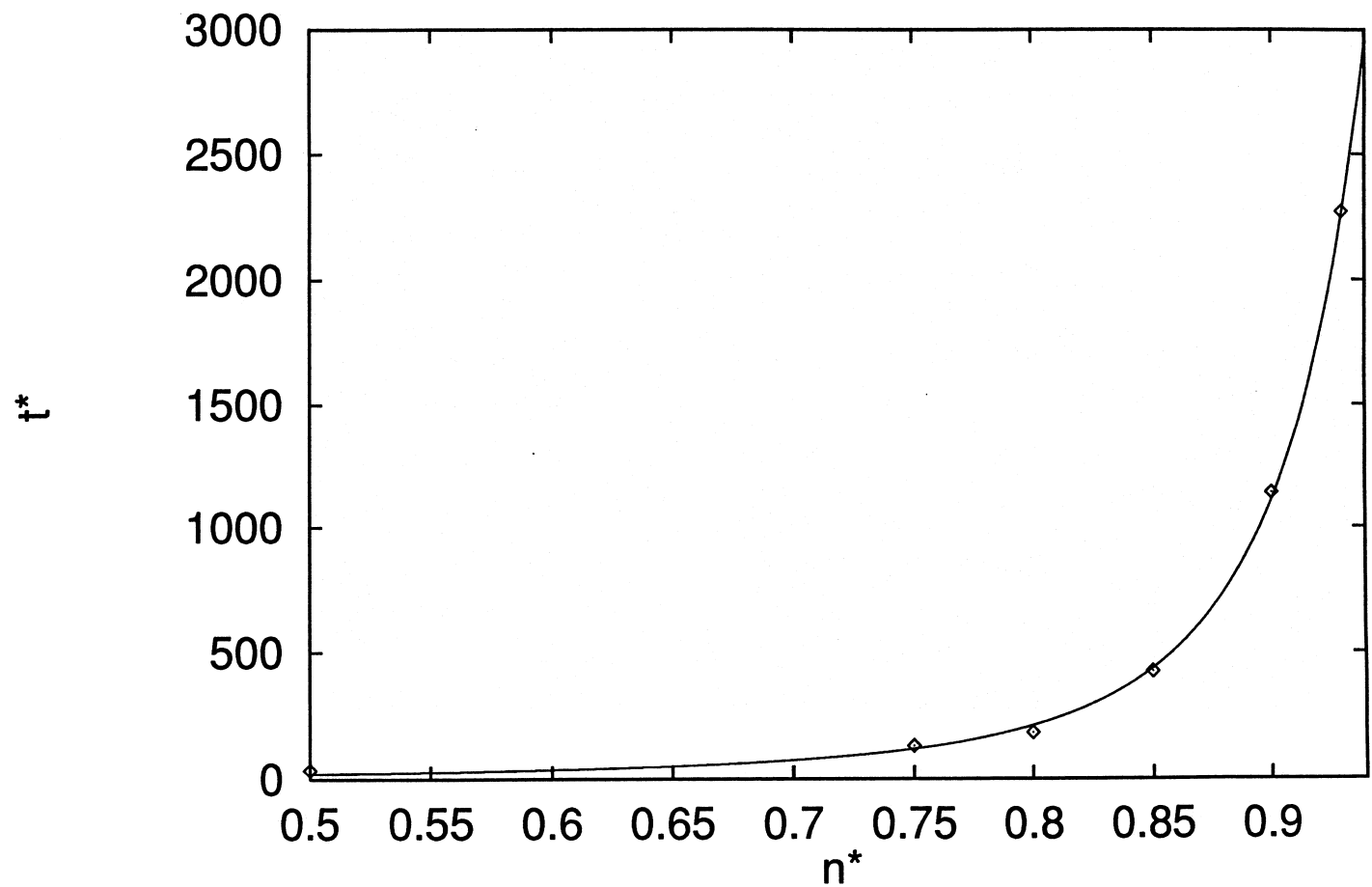
FIGURES

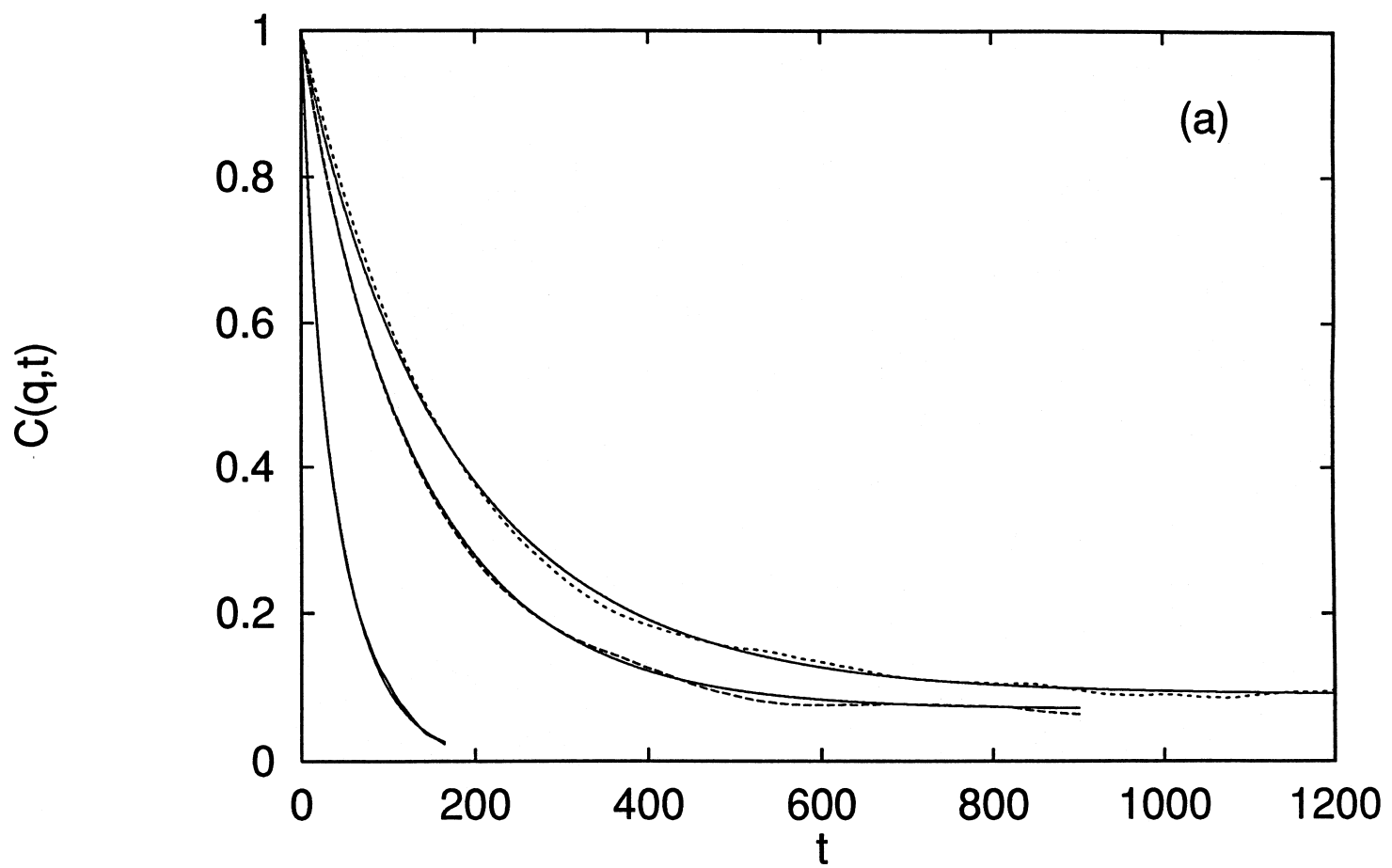
FIG. 1. The characteristic time τ^* as defined in the text, as a function of density n^* . The symbols denote numerical results and the solid line is the best fit to the Vogel-Fulcher form.

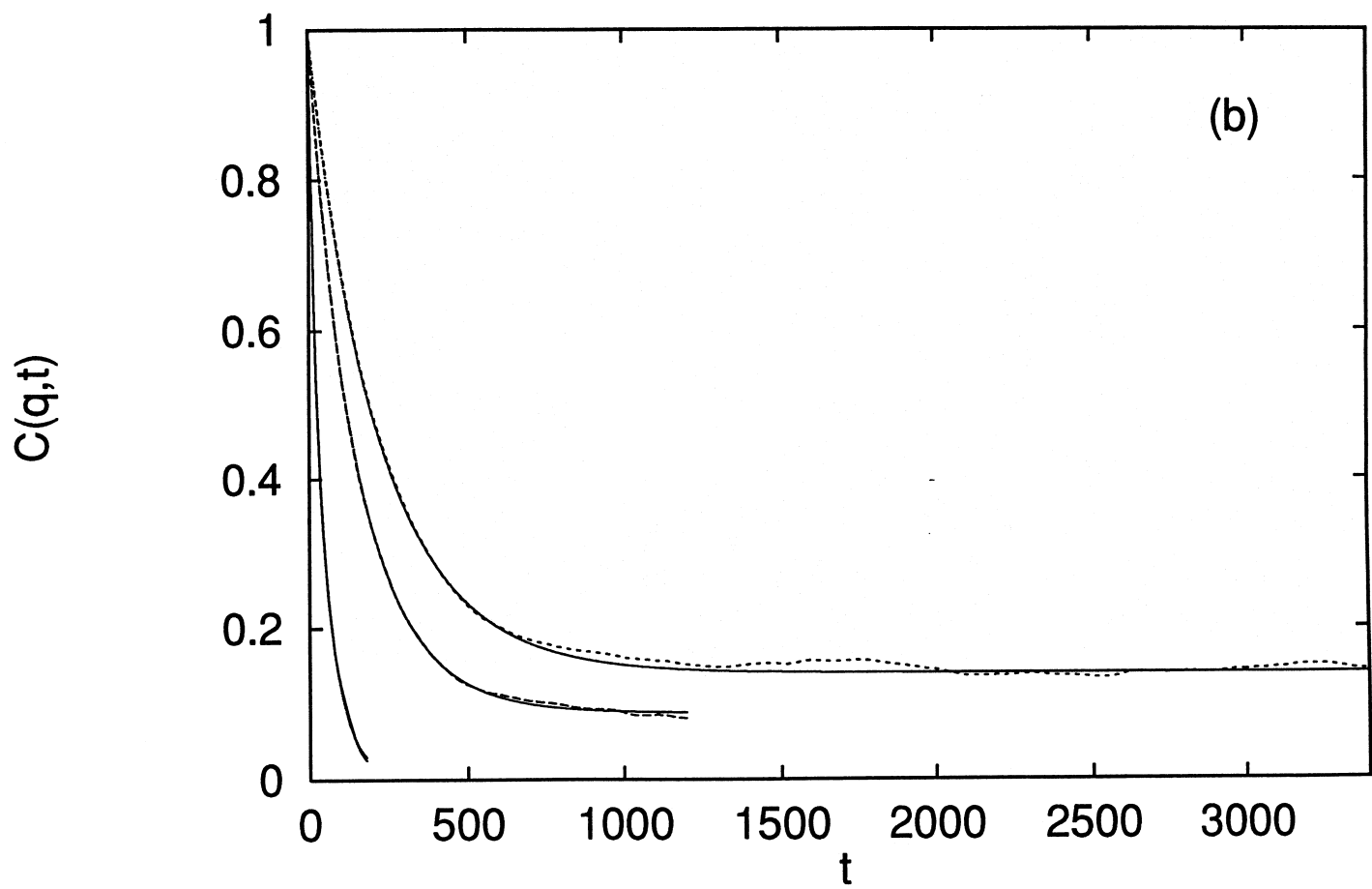
FIG. 2. Normalized, angularly averaged correlation function $C(q, t)$ plotted vs time, for $Q = 14$ (top curve), $Q = 12$ and $Q = 6$ (see text for notation). Results are for $n^* = 0.90$ (panel (a)) and $n^* = 0.93$, (panel (b)). In this and the next Figure the solid curves are the fits and the dashed ones the data.

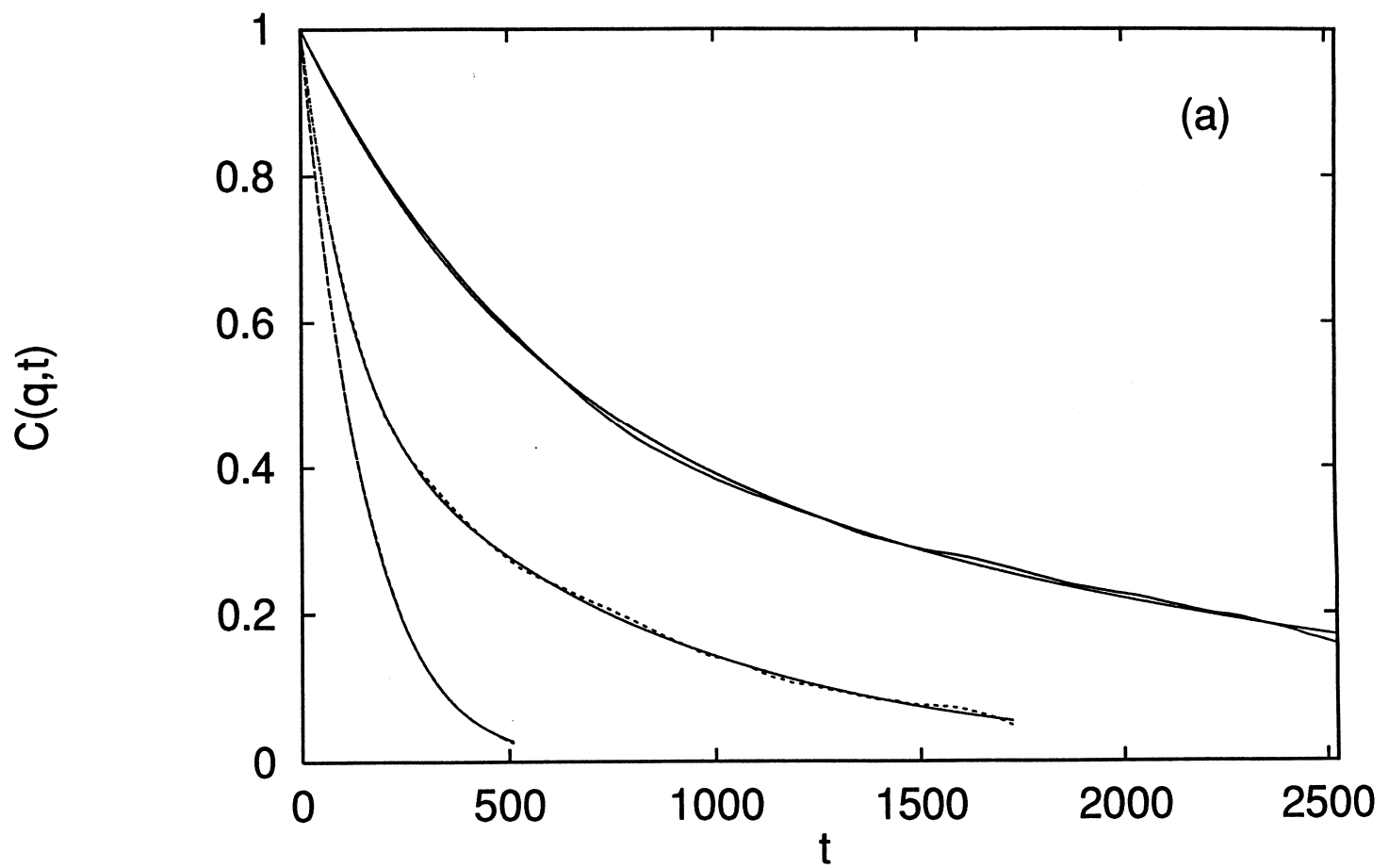
FIG. 3. As in the previous Figure but for $Q = 8$ (top curve), $Q = 13$, and $Q = 10$, (bottom curve).

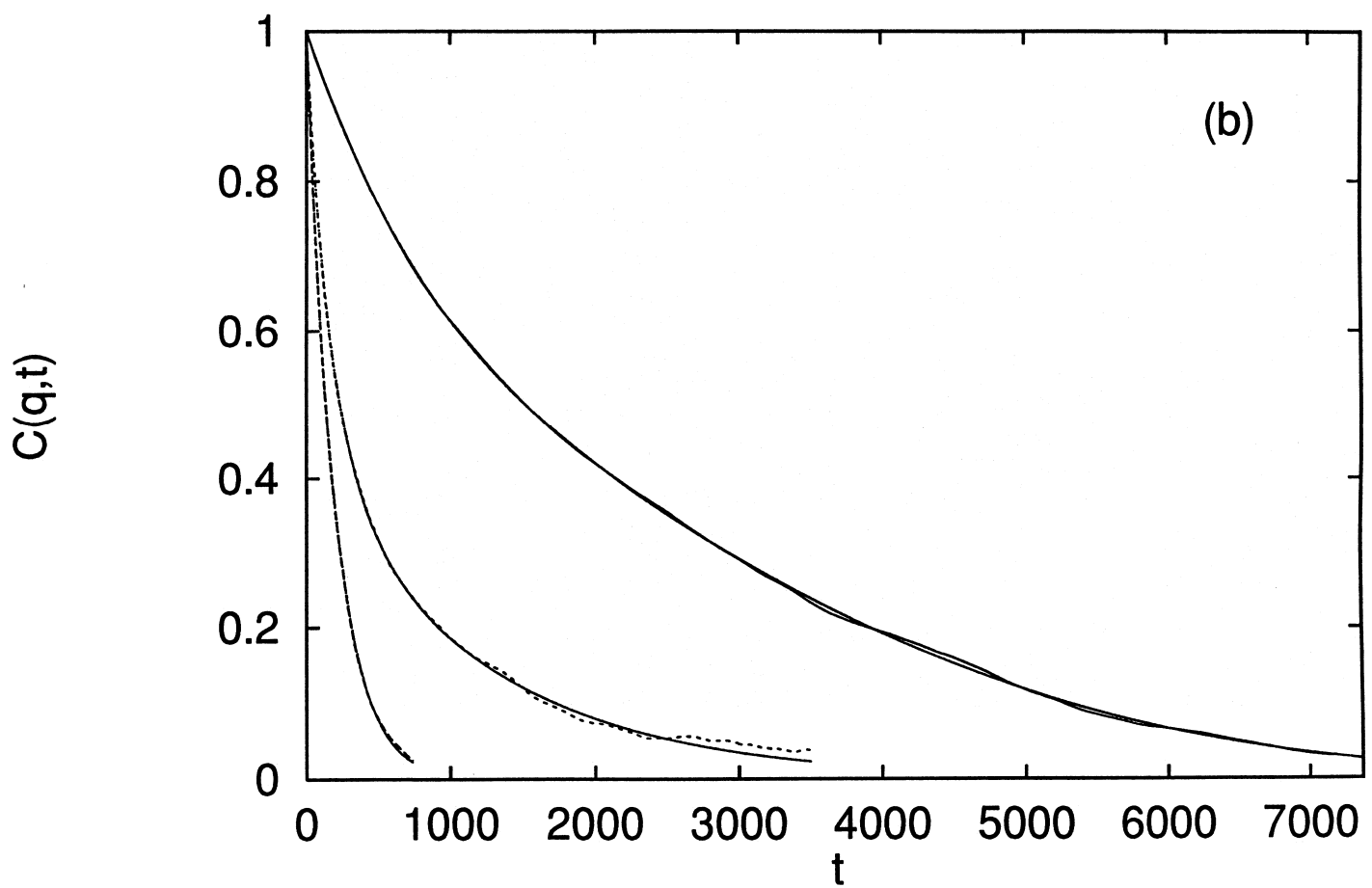
FIG. 4. The characteristic times τ^* (dashed curve) and τ' (symbols) as a function of density.











Characteristic times

